Global Journal of Medical Research: K
Interdisciplinary
Volume 24 Issue 1 Version 1.0 Year 2024
Type: Double Blind Peer Reviewed International Research Journal
Publisher: Global Journals
Online ISSN: 2249-4618 & Print ISSN: 0975-5888

Enhancement of Sensory Quality, Nutritional and Health Benefits of Complementary Baby Food through 2-6μm mid-Infrared Irradiation

By Umakanthan T, Madhu Mathi & Umadevi U

Abstract- Complementary foods are provided to infants when the amount of breast milk produced by the mother is insufficient. Numerous baby foods are available in the market worldwide but their quality is questionable. Therefore, we used our recently invented 2–6μm mid-infrared generating atomizer (MIRGA) on various brands of complementary baby foods to safely enhance their quality in terms of nutrition and sensory attributes. The effects of mid-IR irradiation on baby food included compound transformation, changes in the protein concentration, changes in the chemical bond, and changes in the nanoparticle morphology. The matrix structure and sensory attributes and other benefits were analyzed and validated with various tests and are presented here.

Keywords: MIRGA, 2–6μm mid-infrared, complementary infant food, quality enhancement, food safety, economy.

GJMR-K Classification: FOR Code: 1111

Strictly as per the compliance and regulations of:

Enhancement of Sensory Quality, Nutritional and Health Benefits of Complementary Baby Food through 2–6μm mid-Infrared Irradiation

Umakanthan T [α], Madhu Mathi [σ] & Umadevi U [ρ]

Abstract- **Complementary foods are provided to infants when the amount of breast milk produced by the mother is insufficient. Numerous baby foods are available in the market worldwide but their quality is questionable. Therefore, we used our recently invented 2–6μm mid-infrared generating atomizer (MIRGA) on various brands of complementary baby foods to safely enhance their quality in terms of nutrition and sensory attributes. The effects of mid-IR irradiation on baby food included compound transformation, changes in the protein concentration, changes in the chemical bond, and changes in the nanoparticle morphology. The matrix structure and sensory attributes and other benefits were analyzed and validated with various tests and are presented here.**

Keywords: MIRGA, 2–6μm mid-infrared, complementary infant food, quality enhancement, food safety, economy.

I. Introduction

Breast milk is the ideal food for infants as it has evolved to provide the child with the nutrients needed for growth and development. As the infant grows, the hedonic properties and composition of the breast milk change naturally. This chronological change in the characteristics of the milk fulfills the infant's growth and developmental needs and also encourages the infant to learn new eating skills and preferences *(Institute of Medicine, 1991; Picciano, 2001; Dowey, 2001; Murray, 2017).* Nevertheless, not all infants can obtain all the nutrition they need when the amount of breast milk is insufficient. Hence, the food industry has developed a wide variety of complementary baby foods including baby rice cereals and pureed meats, vegetables, and fruits. However, the quality of marketed complementary baby foods around the world is under debate *(Mohamed et al., 2018).* To complicate this problem, no scientific methods are currently available to improve the quality of complementary baby foods.

In this study, we applied mid-infrared irradiation generated by a mid-infrared generating atomizer (MIRGA) to baby foods, aiming to improve the quality of the foods. The 2–6 μm mid-IR is the safest zone in the infrared spectrum which penetrates obscurant media *(Pereira et al., 2011).* This non-ionizing-irradiated baby foods were subjected to various analyses to determine whether the changes also occurred at the molecular level. The goal was to improve the quality of complementary baby foods without compromising their safety.

II. Materials

MIRGA *(patent No.: 401387)* is a polypropylene plastic atomizer of 20 mL capacity containing an inorganic water-based solution composing Sodium carbonate monohydrate, Sodium carbonate anhydrous, Potassium nitrate and Sodium chloride. The specifications of MIRGA (MIRGA) and the process of generating 2–6µm mid-IR while spraying with MIRGA are described by *Umakanthan et al., 2022a; Umakanthan et al., 2022b; Umakanthan et al., 2023c; Umakanthan et al., 2023d* (Figure S1) *(details presented in Supplementary Text T1)*

Complementary baby foods from three different multinational brands available in the market were individually sprayed with MIRGA, taking care not to mix any brand or batch during the experiments. The samples used were from the same source in terms of the manufacturer and batch number, and the only difference among them was the number of sprayings they received.

The instruments used to identify the changes caused by MIRGA in the complementary baby foods were the following:

FTIR: Fourier-transform infrared spectroscopy (FTIR) was performed using a JASCO 4200 Plus spectrophotometer with ATR (range of 4000–400 cm^{-1} at 298 K). The aim was to detect changes in the chemical bonds.

GC-MS: Gas chromatography-mass spectrometry (GC-MS) was conducted using an Agilent Technologies 7820 GC system with a 5977E MSD, fitted with a DB-5 column. The temperature range was 100–270°C. The carrier gas was helium at a flow rate of 1.2 mL/min. GC-MS analyses revealed chemical compound transformation.

Corresponding Author α: Veterinary hospital, Gokulam Annadhanam Temple Complex, Plot no.: 1684, Meenavilakku-Meenakshipuram Road, Anaikaraipatty Post, Bodinayakanur Taluk, Theni Dt, Tamil Nadu, India. e-mail: rkbuma@gmail.com

Author σ: Veterinary hospital, Vadakupudhu Palayam, Erode Dt, Tamil Nadu, India.

Author ρ: Assistant Professor, Department of Botany, The Standard Fireworks Rajaratnam College for Women, Sivakasi, Virudhunagar (Dt), Tamil Nadu, India.

PXRD: Powder X-ray diffraction (PXRD) was performed using a Rigaku RINT 2500 X-ray diffractometer (CuKα anode; λ = 1.541 Ao). Samples were scanned at 40kV and 30mA from 5 to 35 °C 2θ values and analyzed using PDXL2 software (Rigaku). PXRD analyses revealed structural changes.

TEM: A high-resolution transmission electron microscope (HR-TEM) model FEI –TECNAI G2-20 TWIN was used to observe the sample structure. The operating voltage was 200kV.

Proton NMR: H1 NMR spectra of milk powder samples (ca. 8mg for 1H) in DMSO-D6 (Eurisotop, France) were recorded to identify proton resonances. Spectra were acquired using a 300 MHz AVANCE II (Bruker BioSpin, Switzerland) spectrometer equipped with a 5mm BBO probe (Bruker BioSpin, Switzerland). The experiments were conducted at 298.15 K and data were processed using the standard pulse sequence library of TopSpin 3.2 (Bruker BioSpin, Switzerland). The proton resonance was identified.

3D Fluorescence spectroscopy: 3D fluorescence emission spectra were measured on a Hitachi F-7000 spectrophotometer in the range of 200–700 nm at 298 K. The spectral patterns were analyzed using the original software (Hitachi). The contour and signal-to-noise ratios were determined.

An expert sensory panel (n=6) from the dairy industry and a group of feeding mothers (n=18) participated in the study.

III. Methods

Spraying was done from a 0.25 to 0.50 m distance toward the packaged (polythene/ paper) baby food *(the spraying method is shown in the video link presented in Supplementary Video V1)*. This distance is essential for the MIRGA sprayed solution to form ion clouds, which oscillate generating 2–6μm mid-IR. The rays can penetrate the packaged material and exert their action on the baby food inside. Close spraying does not generate sufficient energy to yield the desired outcome.

A control sample of 50 g was taken from a 500 g polyethylene packet of a specific brand and batch of baby food and a sensory test was carried out. Then, the packet containing the remaining baby food was sealed with cellophane tape, and one MIRGA spraying was externally applied from a distance of 0.25 to 0.50 m. The packet was opened and a sample of 30 g was taken, which was used for another sensory test. The cycle of spraying and sensory tests was repeated 14 times. Second trial was done using another 14 samples taken from a specific second brand and batch of 500 g baby food packet. The same procedure was repeated for a specific third brand and batch of baby food also. The sensory tests were conducted using an acceptability index based on a hedonic scale with a 9-point nominal structure: 1, dislike extremely; 2, dislike very much; 3, dislike moderately; 4, dislike slightly; 5, neither like nor dislike; 6, like slightly; 7, like moderately; 8, like very much; 9, like extremely *(Everitt, 2009; Wichchuki et al., 2014)*. Analyses were repeated for increased accuracy.

The control and 4-, 10-, and 14-sprayed samples were subjected to various laboratory analyses and the obtained results were compared.

IV. Results and Discussion

After MIRGA spraying, the taste and palatability difference among the brands was substantial. Therefore, we limited our analysis and discussion to one complementary baby food made by a multinational company (Table 1).

Table 1: Sensory Attribute Test

Number of MIRGA sprayings	Score by the sensory expert panel	Opinion of feeding mothers
Control	5	Neither like nor dislike
1	5	-
2	6	-
3	6	-
4	7	Like moderately
5	7	-
6	6	-
7	7	-
8	8	-
9	8	-
10	9	Like extremely
11	6	-
12	5	-
13	4	-
14	2	Dislike very much

The control had a regular taste. The samples sprayed 4 and 10 times acquired moderately and highly enhanced sweetness, respectively, but the sweetness of the sample sprayed 14 times was greatly reduced. These changes in sensory attributes were perceived 1–5 minutes after spraying.

GC-MS of complementary baby food

Instrumentation results of Complementary baby food (raw data of all instrumentations presented in Supplementary data D1)

Table 1: Volatiles in complementary baby food, identified by GC-MS analysis

R.T. (Min)	Name of Compound	% Peak area of the samples				
		Control	4-sprayed	10-sprayed	14-sprayed	Remarks
11.15	n-Hexadecanoic acid	0.12	1.66	0.0	0.0	
11.81	n-Hexadecanoic acid	4.32	3.22	0.0	0.0	
11.93	n-Hexadecanoic acid	0.77	5.07	0.0	0.0	
12.06	n-Hexadecanoic acid	0.82	0.61	0.0	0.0	
12.48	11-Dodecen-1-ol trifluoroacetate	0.92	7.25	0.0	0.0	
12.63	n-Hexadecanoic acid	1.28	2.68	0.0	0.0	
12.71	n-Hexadecanoic acid	0.57	3.66	0.0	0.0	
12.81	n-Hexadecanoic acid	0.25	0.0	0.0	0.0	
13.02	n-Hexadecanoic acid	0.74	0.0	0.0	0.0	
13.10	n-Hexadecanoic acid	0.39	0.0	0.0	0.0	
13.28	9-Octadecenoic acid	2.20	0.0	0.0	0.0	
13.49	9-Octadecenoic acid	9.64	0.0	0.0	0.0	
13.59	trans-13-Octadecenoic acid	0.0	26.52	0.0	0.0	*Only present in the 4-sprayed sample.* Anti-inflammatory effects (Hameed*et al.*, 2016)
13.67	2,3,3-Trimethyl-1,7-octadiene	0.0	31.88	0.0	0.0	*Only present in the 4-sprayed sample.* New compound.
14.24	6-Octadecenoic acid	0.19	0.0	0.0	0.0	
14.66	Oleic Acid	0.92	0.0	0.0	0.0	
14.75	9-Octadecenoic acid	1.37	0.0	0.0	0.0	
15.35	Octadec-9-enoic acid	0.14	0.0	0.0	0.0	
15.40	9-Octadecenoic acid	0.26	0.0	0.0	0.0	
15.48	9,17-Octadecadienal	0.94	0.0	0.0	0.0	
15.58	1,1'-(1,3-Propanediyl)bis-cyclohexane	0.0	12.22	0.0	0.0	*Only present in the 4-sprayed sample.* New compound.
15.88	2-Octyl-cyclopropaneoctanal	0.35	0.0	0.0	0.0	
16.19	cis-9-Hexadecenal		0.75	0.0	0.0	
16.23	2-Hydroxy-cyclopentadecanone	2.13	0.0	0.0	0.0	
16.26	cis-9-Hexadecenal	2.71	0.0	0.0	0.0	
16.28	cis-11-Hexadecenal	0.0	1.69	0.51	0.0	
16.44	Oxacyclododecan-2-one	1.43	0.0	0.0	0.0	
16.58	15-Hydroxypentadecanoic acid	8.58	0.0	0.0	0.0	
16.83	Oleic acid	1.25	0.0	0.0	0.0	
16.96	2,3-Dihydroxypropyl elaidate	0.46	0.0	0.0	0.0	
17.12	cis-11-Hexadecenal	0.0	9.75	0.0	0.0	*Only present in the 4-sprayed sample.* New compound.
17.37	cis-Vaccenic acid	0.48	0.0	0.0	0.0	
17.43	Bicyclo[5.3.1]undecan-11-one	0.55	0.0	0.0	0.0	

17.84	Tetradecanal	8.39	0.0	0.0	0.0	
17.84	2-Cyclohexyl-dodecane	0	0.0	44.37	43.04	
17.87	(1-Methylethyl)-cyclohexane	12.09	0.0	0.0	0.0	
18.12	Oleic acid, 3-hydroxypropyl ester	13.07	0.0	0.0	0.0	
18.29	Octadecanoic acid, 2,3-dihydroxypropyl ester	2.28	0.0	0.0	0.0	
18.52	2-Methyl-Z,Z-3,13-octadecadienol	2.20	0.0	0.0	0.0	
18.75	3-Trifluoromethylbenzoic acid, 2-pentadecyl ester	1.31	0.0	0.0	0.0	
18.84	13-Octadecenal	0.5	8.39	0.0	0.0	*Only present in the 4-sprayed sample.* New compound.
19.22	9-Octadecenoic acid (Z)-, 2-hydroxy-1-(hydroxymethyl) ethyl ester	0.32	0.0	0.0	0.0	
19.71	Oleic acid	0.0	9.39	56.14	56.96	*Most abundant in the 10- and 14-sprayed samples.* Antibacterial, anticancer, immune-stimulant, and anti-inflammatory effects (Mustapha *et al.*, 2016; Helioswilton *et al.*, 2013).
19.77	9-Octadecenoic acid (Z)-, 2,3-dihydroxypropyl ester	14.12	0.0	0.0	0.0	
20.02	Fumaric acid, cis-hex-3-enyl heptadecyl ester	2.4	0.0	0.0	0.0	
20.27	9,17-Octadecadienal,	3.2	0.0	0.0	0.0	
20.70	Isopropyl linoleate	0.51	0.0	0.0	0.0	
20.91	9,17-Octadecadienal,	0.74	0.0	0.0	0.0	
21.07	Decylsulfide	1.66	0.0	0.0	0.0	
21.15	9-Octadecenoic acid (Z)-, 2-hydroxy-1-(hydroxymethyl) ethyl ester	0.35	0.0	0.0	0.0	
21.38	1,2,3,6-Tetrahydro-1-methyl-4-phenyl-pyridine	0.24	0.0	0.0	0.0	
21.76	9-Octadecenoic acid (Z)-, 2-hydroxyethyl ester	1.16	0.0	0.0	0.0	

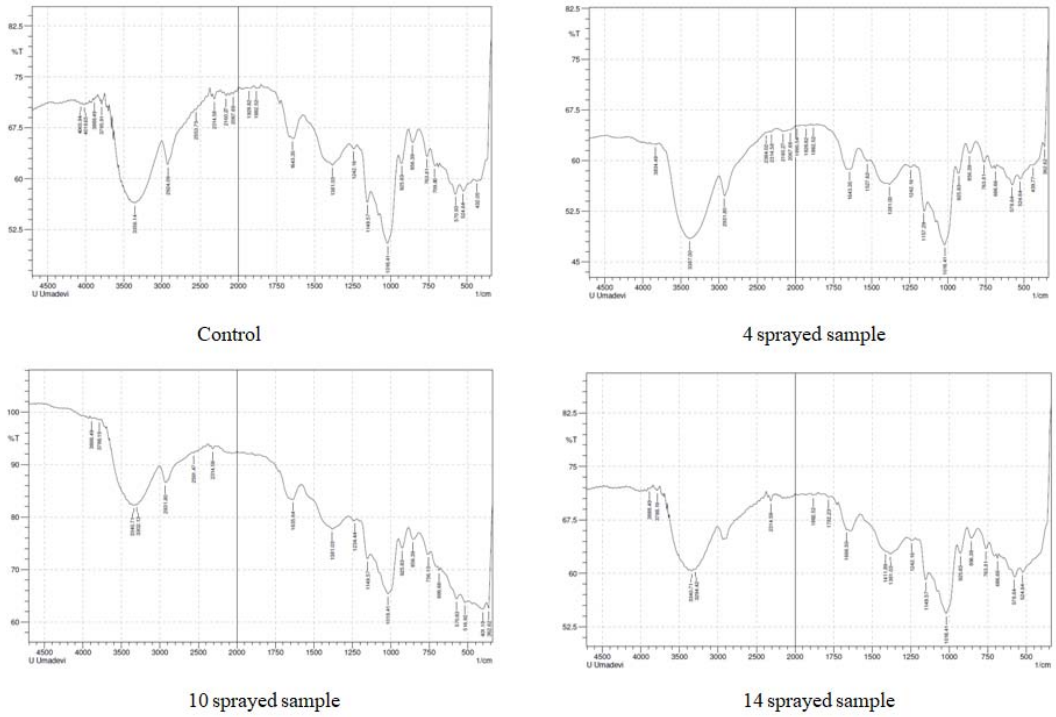

Fig. 1: GC-MS spectra of complementary baby food

The control sample contained many aldehydes and long-chain fatty acids such as oleic acid and palmitic acid. After spraying the samples 4 and 10 times, the sweetness increased and the long-chain fatty acid content, which has health benefits, increased *(Zárate et al., 2017; Hoppen brouwers et al., 2019).* In particular, the long-chain fatty acid6-octadecenoic acid (C18) and 2-cyclohexyl-dodecane were generated by spraying. The sample sprayed 14 times showed oleic acid and 2-cyclohexyl-dodecane as the major peaks. These compounds are the by-products of spraying and transformation (Figure 1, Table 1).

MIRGA spraying has been reported to increase the content of some free fatty acids, which influence the product quality, flavor, texture, and nutritional properties *(Larodan Research Grade Lipids; Human Metabolome Database)* and as a consequence, also shows health benefits *(Kilcawley et al., 2017).* The samples sprayed 10 and 14 times showed oleic acid as the most abundant compound. This fatty acid has many health benefits like increasing high density lipoprotein, reducing the risk of heart diseases, etc. *(Aleksandra et al., 2019; Anka et al., 2021)*

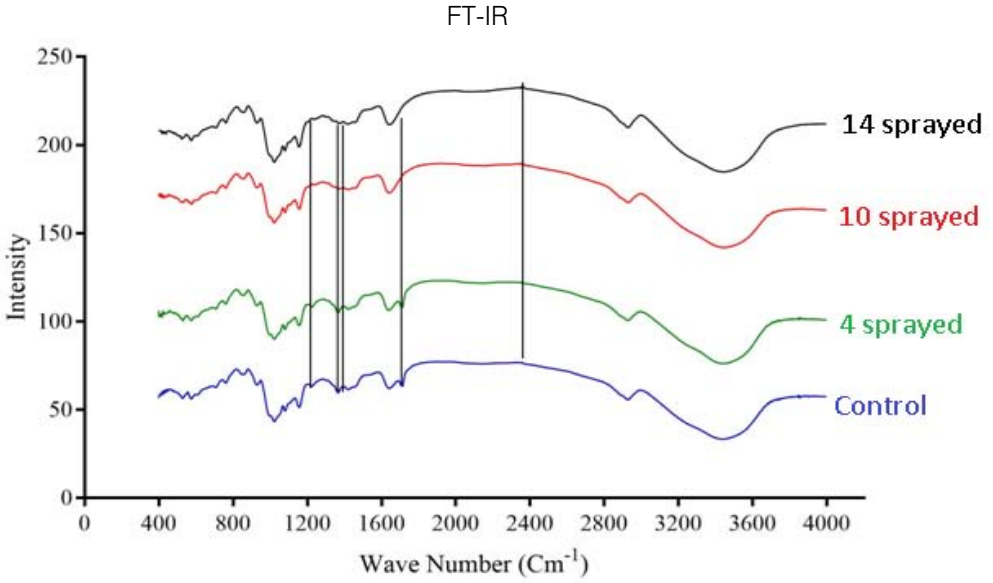

Fig 2: FTIR of complementary baby food

S-H bond stretching was observed near 2358 cm^{-1} *(Merck, 2020)* in the 10- and 14-sprayed samples, which suggests the breakage of the protein secondary structure due to the reduction of the disulfide bonds. Furthermore, the control and the 4-sprayed sample did not show any change in their protein structures. However, these two samples showed an aliphatic C=O stretching at 1700 cm^{-1} from carboxylic acid, which is most probably derived from lipids. This signal was absent in the 10- and 14-sprayed samples, which may be due to the formation of lipid anhydrides *(Merck, 2020).* C-N bond stretching was detected at 1395 cm^{-1}, which corresponded to free amino acids. The intensity of the C-N bond stretching signal waslower in the samples sprayed 10 and 14 times, indicatingthe formation of amino acid dimers *(Rumbley et al., 2001; Kazlauskas, 2018).* C-O bond stretching was observed at 1350 $cm^{-1}$for the control and the sample sprayed 4 times but it was absent in the samples sprayed 10 and 14 times. This may be explained bythe breakage of lactose into glucose and galactose (Figure 2). The increase in the sweetness of the sample sprayed10 timeswas be due to the formation of glucose from lactose *(Vernikovskaya et al., 2022).* As glucose is much sweeter than lactose, the breakage of lactose caused the increased sweetness of the baby food. However, the decreased sweetness in the sample sprayed14 times wasdue to the degradation of the baby food caused by excessive spraying.

Another C-N bond stretching was detected at 1220 cm^{-1} (Fig 2), which corresponded to the free amino acids *(Merck, 2020).* This signal was present in the control and the sample sprayed4 times but was absent in the samples sprayed10 and 14 times. This may be explained bythe formation of amino acid dimers at the amine group in the samples sprayed10 and 14 times.

PXRD

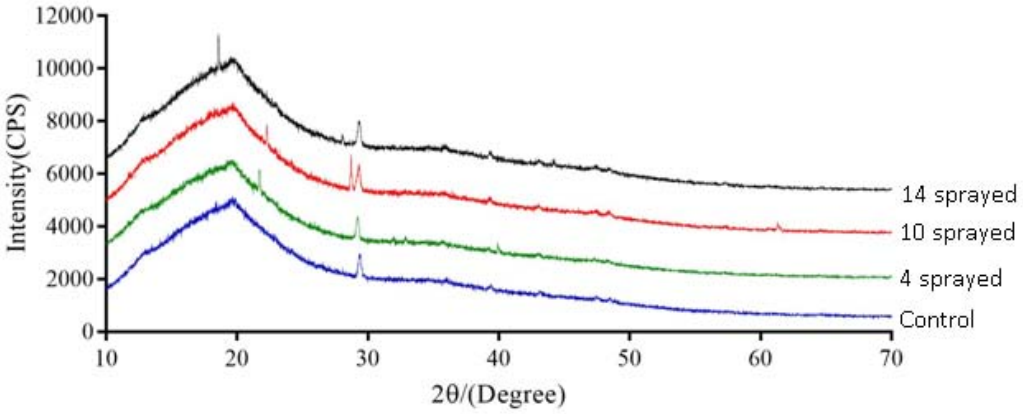

Fig. 3: PXRD of complementary baby food

All four (control, 4, 10 and 14 sprayed) samples showed a single broad peak at 19.6°. This result suggests an improvement in the crystallinity of the powders as the number of sprayings increased. However, the crystallinity of the sample sprayed 4 times decreased by 6.8% because of the formation of lipid anhydrides *(Herman, 2007).* On the other hand, the crystallinity of the samples sprayed 10 and 14 times increased by 5.9% and 9.9%, respectively (Table 2).

Table 2: PXRD analysis of complementary baby food

Percentage change in the baby food samples				
	Control	4-sprayed	10-sprayed	14-sprayed
Peak (min)	19.64	19.33	19.68	18.58
Area	111837	104215	118457	122864
Change in area	0	-7622	6620	11027
Fraction change in area	0	-0.06815	0.059193	0.098599
Percentage change	0	-6.81528	5.919329	9.859885

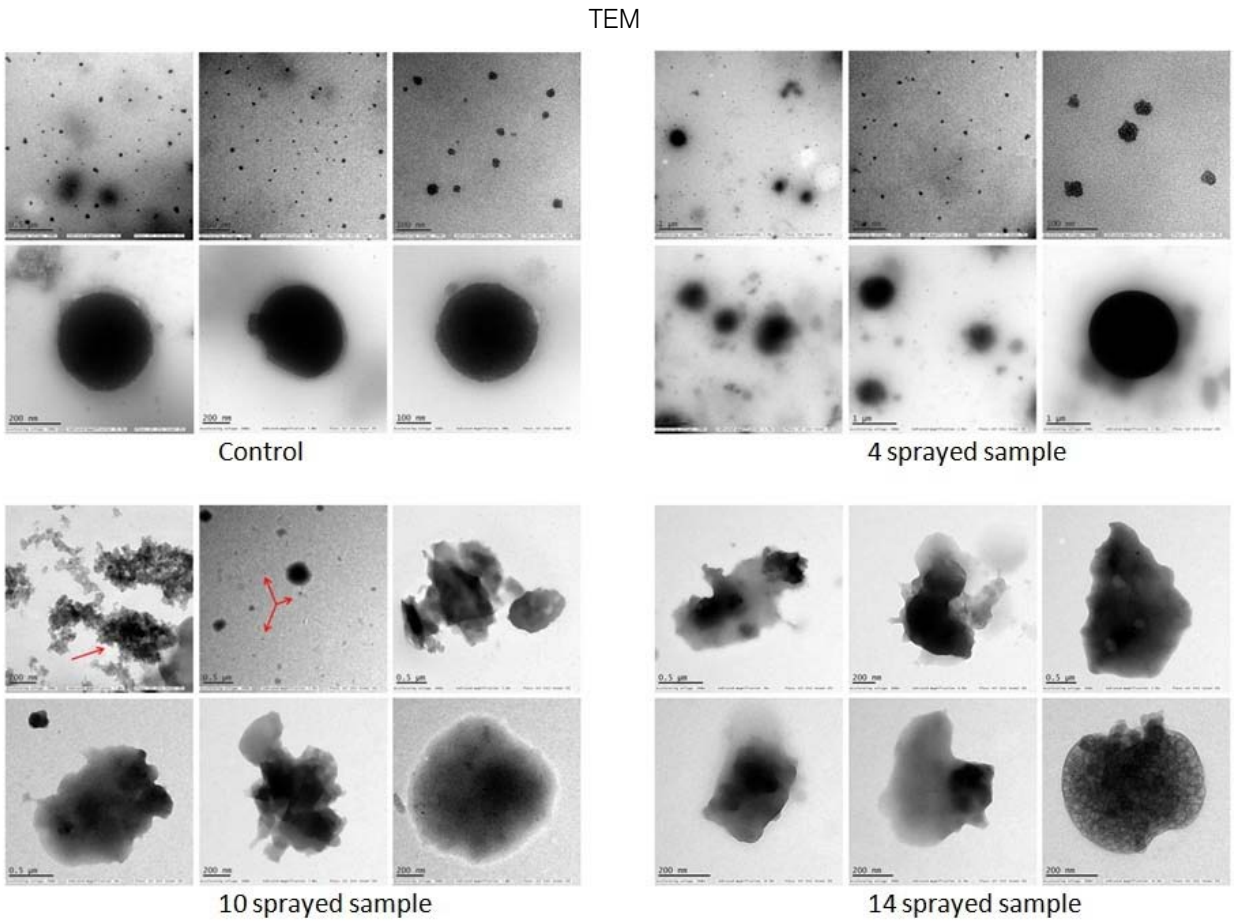

Fig. 4: TEM of complementary baby food

Table 3: TEM analysis of complementary baby food

	Control	4-sprayed	10-sprayed	14-sprayed
Size of the particles	Nanoparticles of 10–30 nm and sub-micron particles of 300–400 nm	Nanoparticles of 10–30 nm and larger sub-micrometer and micrometer-sized particles of 100–400 nm	Nanoparticles of 10–40 nm and amorphous-like aggregates of 0.5–2 μm	Different mass aggregates in the 0.5–2 μm range
Shape of the particles	Mainly semi-spherical	Mainly semi-spherical	Clustered. Ellipsoidal and amorphous-like aggregates	Mass aggregates
Particle distribution	Nanoparticles were unevenly distributed. Larger particles showed a homogeneous mass distribution	Nanoparticles were unevenly distributed. Larger particles showed a homogeneous mass distribution	Uneven distribution of the mass within the aggregate body	Uneven mass distribution within the aggregate body

Compared to the control, the sample sprayed 4 times showed minor changes to the morphology and matrix structure. By contrast, the samples sprayed 10 and 14 times showed substantial changes to the morphology and matrix structure, with differences mainly in the type of particles observed. In the control and 4-sprayed samples, the main components were semi-spherical individual nanoparticles and sub-micrometer particles, whereas in the samples sprayed 10 and 14 times, ellipsoidal nanoparticles were grouped in large clusters and micrometer-sized mass aggregates were observed (Table 3) *(details presented in Supplementary Text T2).*

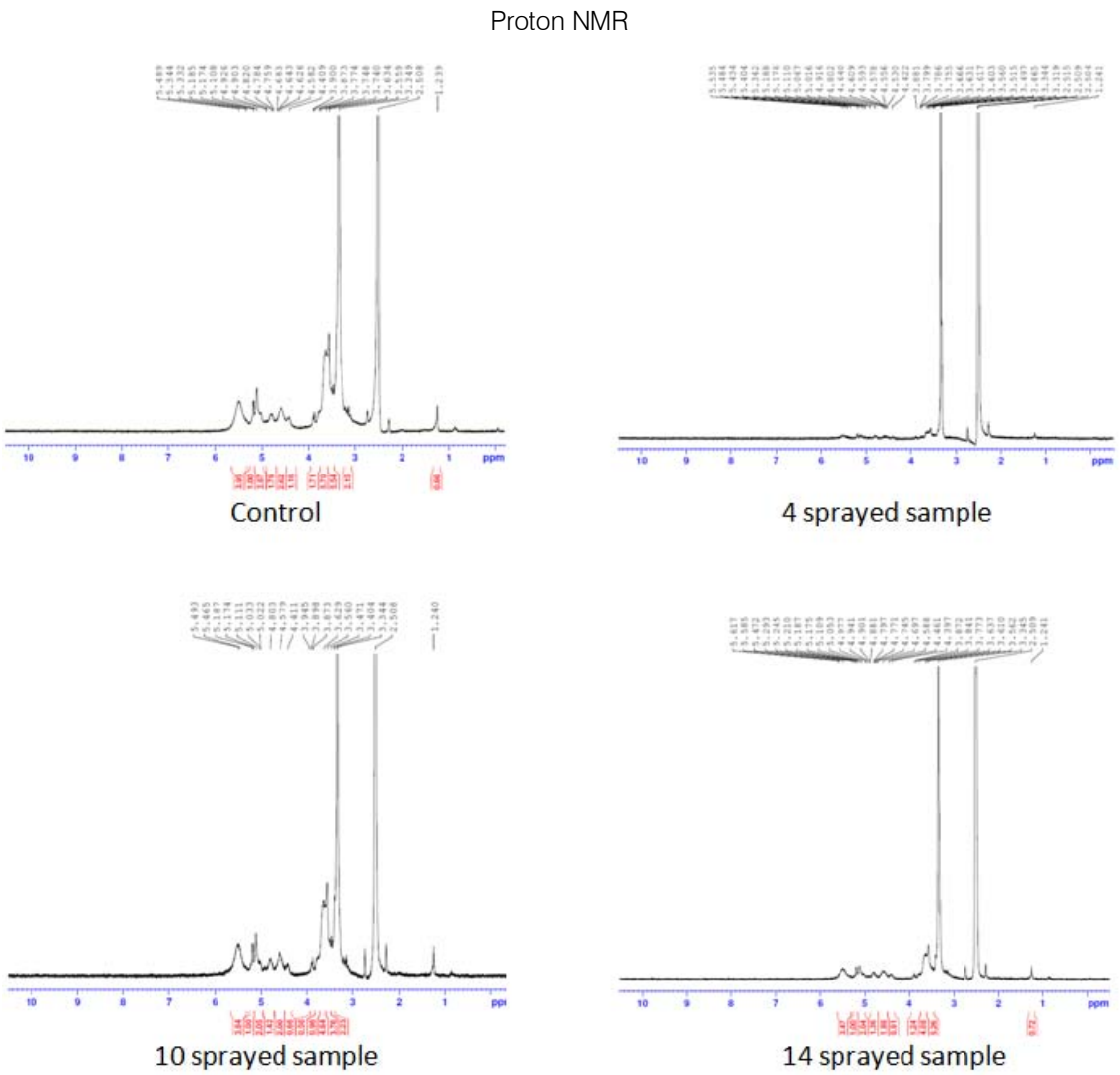

Fig. 5: 1H-NMR of complementary baby food

The intensity of the peak at δ 3.90–6.00 was due to the –OH and –NH protons of the sugar ring, and that at δ 1.068–1.103 was due to the β-hydroxy butyrate group. This group has potent anti-inflammatory property, hence useful in inflammatory bowel disease and irritable bowel syndrome. This peak was notable in the sample sprayed10 times, small in the sample sprayed 14 times, and absent in the sample sprayed4 times (Figure 5). These differences in peak intensities were related to the varying protein solution concentration that resulted from the changes induced by MIRGA spraying *(details are presented in Supplementary Text T3).*

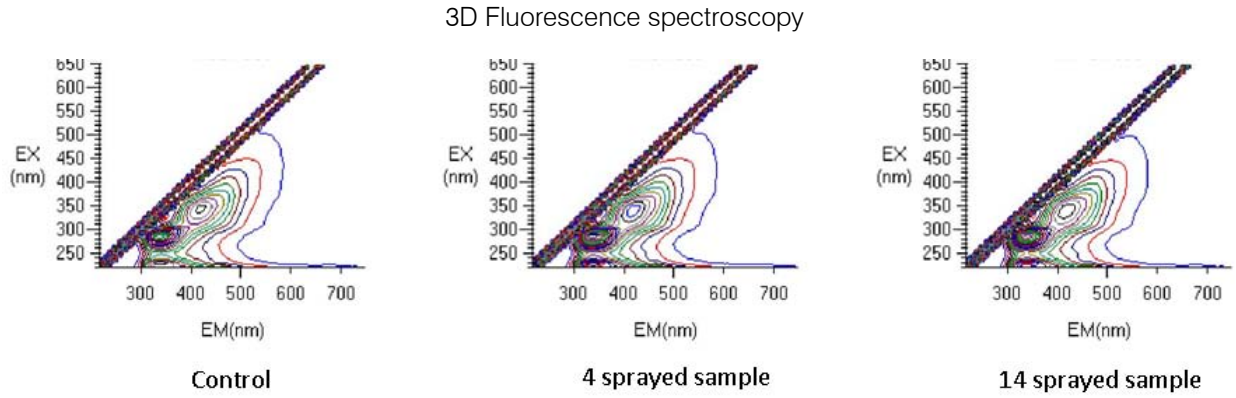

Fig. 6: 3D Fluorescence spectroscopy of complementary baby food

The samples were fluorescence active. A Rayleigh scattering peak ($\lambda_{ex}=\lambda_{em}$) was observed in all spectra. The increased fluorescence intensity in the sample sprayed14 times was due to the spectral behavior of the tryptophan residues that were formed as a result of the unfolding of the protein *(Kazlauskas, 2018; Rumbley et al., 2001)* (Figure 6). Tryptophan is useful for *in vivo* synthesis of proteins, to cure of autism, cognitive dysfunction, cardiovascular and kidney diseases, inflammatory bowel diseases and induce sleep, etc.

MIRGA and mid-infrared irradiation

The concept of MIRGA is based on the action of the2–6 μm mid-IR irradiation on the chemical bonds of coffee, tea, cocoa powder, edible salt and terminalia as described in previous studies conducted by our team *Umakanthan et al., 2022a; Umakanthan et al., 2022b; Umakanthan et al., 2023c; Umakanthan et al., 2023d (a detailed discussion is presented in Supplementary Text T4)*.

Action of MIRGA-emitted 2–6 μmmid-IR on baby food

The laboratory analyses described above showed that the C–N and C–O bond stretching, formation of new molecules, lactose breakage, increased crystallinity, and configurational changes were responsible for the improved quality of the baby food. The applied mid-IR is absorbed by the carbohydrates, protein, fat, and water in the food. The vibrational frequencies of these molecules correspond to this wavelength *(Toor et al., 2018),* thus resulting in photostimulation and photobiomodulation *(Pollack, 2015).* These phenomena lead to changes in the vibrational modes of the molecules (e.g., stretching) *(Mohan, 2004; Shankar, 2017)* and chemical compound transformation *(Xu et al., 2017),* ultimately altering the physical and chemical properties *(Yi, 2012; Atkins et al., 2011)* of the food. Thus, the favorable organoleptic and biochemical changes corresponded to the number of sprayings occurred.

FTIR analysis revealed that the reduction of disulfide bonds results in health benefits *(Mossuto, 2013).* Moreover, the breakage of lactose into glucose ad galactose increased the sweetness of the food. Fetuses *(Hayes et al., 2017),* infants, and children naturally prefer the sweet taste *(Murray, 2017)* so sweeter baby food is expected to be more appealing to infants.

The formed lactose-free by-product is suitable for lactose-intolerant infants and is also an affordable alternative to Maltodex *(Maldonado et al., 1998; Hofman et al., 2015)* as well as a therapeutic agent against diarrhea in children *(Sethi et al., 2018).* As evidenced by the PXRD analysis, increased crystallinity is an added value to the manufacturer and consumer. 3D fluorescence spectroscopy revealed the unfolding of protein as a result of the MIRGA spraying, with more sprayings resulting in greater unfolding. By contrast, FTIR revealed that 4 spraying preserved the protein structure. Based on our experience, we consider the complementary baby food enhanced by MIRGA spraying can be used in addition to breast milk feeding when the latter is insufficient. Also based on our experience in this research and unrevealed results in this paper, we humbly request feeding mothers to feed babies with the mother's milk or on deficit the cow milk especially milk of native cows or the MIRGA sprayed complementary baby foods.

V. Conclusion

Complementary baby food was irradiated with 2–6μm mid-infrared. Sensory and instrumental analyses revealed that mid-IR irradiation favorably altered the chemistry of complementary baby food, thereby improving the aroma, texture, nutritional, and health benefits of the baby food. This technology can be used in the future to enhance the quality and sensory attributes of similar products.

Funding

The authors received no specific funding for this study.

Author contributions

Umakanthan: Conceptualization, Methodology, Supervision, Validation.
Madhu Mathi: Data curation, Investigation, Visualization, Writing - Original draft preparation.
Umadevi: Project administration, Resources
Umakanthan, Madhu Mathi: Writing- Reviewing and Editing.

Conflict of interest

In accordance with the journal's policy and our ethical obligation as researchers, we submit that the authors Dr. Umakanthan and Dr. Madhu Mathi are the inventors and patentee of Indian patent for MIRGA *(under-patent no.: 401387)* which is a major material employed in this study.

Data and materials availability

All data is available in the manuscript and supplementary information.

References Références Referencias

1. Institute of medicine: Nutrition During Lactation. Washington, DC, National Academy press, 1991.
2. Picciano, M.F. Nutrient composition of human milk. Pediatric Clin. North Am. 4853-67, 2001.
3. Dewey, K.G. (2001). Nutrition Growth and Complementary feeding of The Breast Feed Infant. Pediatric clinics of North America, 48(1), 87-104; doi: 10.1016/s0031-3955(05) 70287-X
4. Murray, R. D. (2017). Savoring Sweet: Sugars in Infant and Toddler Feeding. Annals of Nutrition and Metabolism, 70(3), 38–46. doi:10.1159/000479246

5. Mohamed, E., Adel, Alajtal., Nada, Alsedawi., H., G., M., Edwards. (2018). Nutritional Evaluation of Some Commercial Infant Formula Consumed in Misurata-Libya. doi: 10.26538/TJNPR/V2I1.11
6. Pereira M F, Shulika O, 2011. Terahertz and MidInfrared Radiation: Generation, Detection and Applications. Springer Science + Business Media B.V., The Netherlands. DOI: 10.1007/978-94-007-0769-6.
7. Umakanthan, Mathi M, 2022a. Decaffeination and improvement of taste, flavor and health safety of coffee and tea using mid-infrared wavelength rays. Heliyon, e11338, Vol 8(11). doi: 10.1016/j.heliyon.2022.e11338
8. Umakanthan T, Mathi M, 2022b. Quantitative reduction of heavy metals and caffeine in cocoa using mid-infrared spectrum irradiation. Journal of the Indian Chemical Society, Vol 100 (1). doi: 10.1016/j.jics.2022.100861.
9. Umakanthan, T., &Mathi, M. (2023c). Increasing saltiness of salts (NaCl) using mid-infrared radiation to reduce the health hazards. Food Science & Nutrition, 11, 3535–3549. https://doi.org/10.1002/fsn3.3342
10. Umakanthan, Madhu Mathi, 2023d. Potentiation of Siddha medicine using Muppu (Universal Potentiator). International Journal of Pharmaceutical Research and Applications Volume 8, Issue 4 July-Aug 2023, pp: 2070-2084.
11. Everitt, M. (2009). Consumer-Targeted Sensory Quality. Global Issues in Food Science and Technology, 117–128. doi:10.1016/b978-0-12-374124-0.00008-9.
12. Wichchukit S, O'Mahony M. (2014). The 9-point hedonic scale and hedonic ranking in food science: some reappraisals and alternatives. Journal of the Science of Food and Agriculture, 95(11), 2167–2178. doi:10.1002/jsfa.6993
13. Hameed, I., Altameme, H., & Mohammed, G. (2016). Evaluation of Antifungal and Antibacterial Activity and Analysis of Bioactive Phytochemical Compounds of Cinnamomum Zeylanicum (Cinnamon Bark) using Gas Chromatography-Mass Spectrometry. Oriental Journal of Chemistry, 32(4), 1769–1788. doi:10.13005/ojc/320406
14. Mustapha N. Abubakar and Runner R. T. Majinda. GC-MS Analysis and Preliminary Antimicrobial Activity of Albiziaadianthifolia (Schumach) and Pterocarpusangolensis (DC). Medicines 2016, 3, 3; doi: 10.3390/medicines3010003
15. Helioswilton S C, de Souza P R, Peghini B C, da Silva J S, Cardoso C R. An Overview of the Modulatory Effects of Oleic Acid in Health and Disease. Mini-Reviews in Medicinal Chemistry, 2013, 13, 000-000
16. Zárate, R., el Jaber-Vazdekis, N., Tejera, N., Pérez, J. A., & Rodríguez, C. (2017). Significance of long chain polyunsaturated fatty acids in human health. Clinical and Translational Medicine, 6(1). doi:10.1186/s40169-017-0153-6.
17. Hoppenbrouwers, T., CvejćHogervorst, J. H., Garssen, J., Wichers, H. J., &Willemsen, L. E. M. (2019). Long Chain Polyunsaturated Fatty Acids (LCPUFAs) in the Prevention of Food Allergy. Frontiers in Immunology, 10. doi: 10.3389/fimmu.2019.01118.
18. Larodan Research Grade Lipids, https://www.larodan.com/product/13z-octadecenoic-acid/
19. Human Metabolome Database, http://www.hmdb.ca/metabolites/HMDB0041480
20. Kilcawley K N, Mannion D T, (June 21st 2017). Free Fatty Acids Quantification in Dairy Products, Fatty Acids, Angel Catala, IntechOpen, DOI: 10.5772/intechopen.69596. Available from: https://www.intechopen.com/books/fatty-acids/free-fatty-acids-quantification-in-dairy-products.
21. Aleksandra, A., Ana, Stojanovic., Milena, Mikic. (2019). Oleic Acid - Health Benefits and Status in Plasma Phospholipids in the Serbian Population. Serbian Journal of Experimental and Clinical Research, doi: 10.1515/SJECR-2017-0077
22. Anka, T, Petkoska., Anita, Trajkovska-Broach. (2021). Health Benefits of Extra Virgin Olive Oil. doi: 10.5772/INTECHOPEN.96570
23. Merck & Co. Inc. 2020. "You Can Control Your Cholesterol: A Guide to Low-Cholesterol Living". Archived from the original on 2009-03-03. Retrieved 2009-03-14.
24. Rumbley, J., Hoang, L., Mayne, L., & Englander, S. W. (2001). An amino acid code for protein folding. Proceedings of the National Academy of Sciences, 98(1), 105–112. doi: 10.1073/pnas.98.1.105
25. Kazlauskas, R. (2018). Engineering more stable proteins. Chemical Society Reviews. doi: 10.1039/c8cs00014j
26. A., E., Vernikovskaya.,Nitzan, Dubovski., Yaron, Ben, Shoshan-Galeczki., Einav, Malach., Masha, Y., Niv. (2022). Taste and chirality: l-glucose sweetness is mediated by TAS1R2/TAS2R3 receptor. Food Chemistry, doi: 10.1016/J.FOODCHEM.2021.131393
27. Herman F. Mark, Encyclopedia of Polymer Science and Technology, Concise, 3rd edition, John Wiley & Sons, 2007.
28. Toor F, Jackson S, Shang X, Arafin S, Yang H. Mid-infrared Lasers for Medical Applications: introduction to the feature issue. Biomed Opt Express. 2018 Nov 15; 9(12): 6255-6257. doi: 10.1364/BOE.9.006255. PMID: 31065426; PMCID: PMC6491011.
29. Pollack G H. (2015). Cell Electrical Properties: Reconsidering the Origin of the Electrical Potential. Cell Biology International. 39. 10.1002/cbin.10382.

30. Mohan J. Organic Spectroscopy: Principles and Applications, 2nd edition, Alpha science international Ltd., Harrow, UK, 19, (2004). Available at: https://books.google.co.in/books?id=fA08Uy5DR0QC&printsec=frontcover&dq=Jag+Mohan.+Organic+Spectroscopy:+Principles+and+Applications&hl=en&sa=X&ved=0ahUKEwjHpcHUi9fgAhXXFIgKHXvRCpIQ6AEIKjAA#v=onepage&q=Jag%20Mohan.%20Organic%20Spectroscopy%3A%20Principles%20and%20Applications&f=false
31. Shankar D R, 2017. Remote Sensing of Soils. Germany: Springer-Verlag GmbH, p268.
32. Xu R, Xu Y, 2017. Modern Inorganic Synthetic Chemistry, 2nd edn., Elsevier B.V, Netherlands, UK, USA, p124.
33. Yi G C, 2012. Semiconductor Nanostructures for Optoelectronic Devices: Processing, Characterization and Applications. Berlin, Heidelberg: Springer-Verlag, p198.
34. Atkins P, Paula J, 2011. Physical Chemistry for the Life Sciences, Oxford university press, Oxford, p365.
35. Mossuto, M. F. (2013). Disulfide Bonding in Neurodegenerative Misfolding Diseases. International Journal of Cell Biology, 2013, 1–7. doi:10.1155/2013/318319.
36. Hayes, J. E., & Johnson, S. L. (2017). Sensory Aspects of Bitter and Sweet Tastes During Early Childhood. Nutrition Today, 52(Supplement), S41–S51. doi:10.1097/nt.0000000000000201.
37. Maldonado, J., Gil, A., Narbona, E., & Molina, J. A. (1998). Special formulas in infant nutrition: a review. Early Human Development, 53, S23–S32. doi:10.1016/s0378-3782(98)00062-0.
38. Hofman, D. L., van Buul, V. J., & Brouns, F. J. P. H. (2015). Nutrition, Health, and Regulatory Aspects of Digestible Maltodextrins. Critical Reviews in Food Science and Nutrition, 56(12), 2091–2100. doi:10.1080/10408398.2014.940415.
39. Sethi, G., Sankaranarayanan, S., & Sukhija, M. (2018). Low lactose in the nutritional management of diarrhea: Case reports from India. Clinical Epidemiology and Global Health. Vol 6 (4), pg 160-162. doi:10.1016/j.cegh.2018.02.002.

Acknowledgement

Authors thank multi-Faculty scientists of different labs, institutions, universities, etc., around the world for their technical guidance and help; also thank Dr.George Tranter, Chiralabs Ltd., Begbroke Centre for Innovation & Enterprise, Oxfordshire, UK; Dr.Jan IC Vermaak, Manager of Engineering, Nuclear Science Center - Texas A&M University, USA; Dr. Takashiro Akitsu, Professor, Department of Chemistry, Faculty of Science, Tokyo University of Science, Japan; Dr. Kam-Hung Low, X-ray Facility manager, Department of Chemistry, The University of Hong Kong; Ms. Satitaphorn Sriphuttha, Tokyo University of Science, Jap an; Ms. Shiho Murakami, Mr. Kanai and other Spectroscope specialists of Hitachi High-Tech, Japan; Mr. Gary Powell, Lightwind corporation, Petaluma, California, USA; Dr. Senthil Kumar Rajendran, Cell Biology, Biosciences, ÅboAkademi Univesity, Finland; Dr. Ramakrishnan, Head, Indian Veterinary Research Institute, Mukteshwar, India; Dr. R Prabhakaran, Assistant Professor, Department of Chemistry, Bharathiar University, Coimbatore, India; Prof. Dr. Haluk Yucel, Institute of Nuclear Sciences of Ankara University, Tandogan Yerleskesi, 06100, Ankara, Turkey; Dr. Anuradha Das, NISER, Bhubaneshwar; Dr. Carlos Romero, Carabobo State University, Venezuela; Ms. Becky Gee, Scientific consultant, Unites States; and other Kolabtree experts; All financiers who funded this research for nearly 2 decades; And we would also like to apologize to all scientists and other helpers around the world who are not cited here now.

Supplementary Data

D1: Raw data files of Complementary baby food instrumentations
https://drive.google.com/open?id=1Y31W6KDDz3jveY2GPB8P3x3U4-T8KEw8

Supplementary video:

V1: Method of spraying
https://drive.google.com/open?id=1QoRwTESKfSdoJTfD--xlG9YpTDnVonGW

Supplementary Text

T1:

MIRGA *(under-patent no.: 401387)*is a 20-mL capacity polypropylene plastic atomizer containing an inorganic (molar mass 118.44 g/mole) water-based solution. The sprayer unit has dimensions 86 × 55 × 11 mm, an orifice diameter of 0.375 mm, ejection volume 0.062 ± 0.005 mL, and ejection time 0.2 s. The average pressure is 3900 Pa, and the cone liquid back pressure is 2000 N/m^2. During spraying, approximately 1-μg weight of water is lost as mist and the non-volatile material in the sprayed liquid has a concentration of 153 mg/mL. Depending on the pressure applied to the plunger, every spraying is designed to generate 2–6 *μ*m as estimated by an FTIR (retro-reflector) interferometer instrument (Detector type D* [cm HZ1/2 - 1] MCT [2-TE cooled]) at Lightwind, Petaluma, CA, USA.

Raw data files for estimation of 2-6 μm mid-IR generated from MIRGA while spraying: https://drive.google.com/open?id=1zTiqlOIWVgpaTsiEFqGeyvDM62juHM06

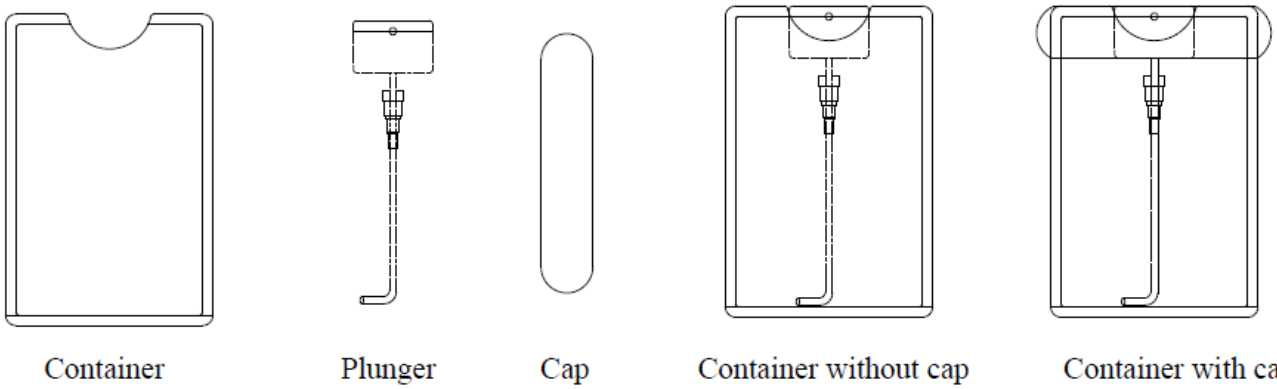

Fig: Parts of the MIRGA sprayer

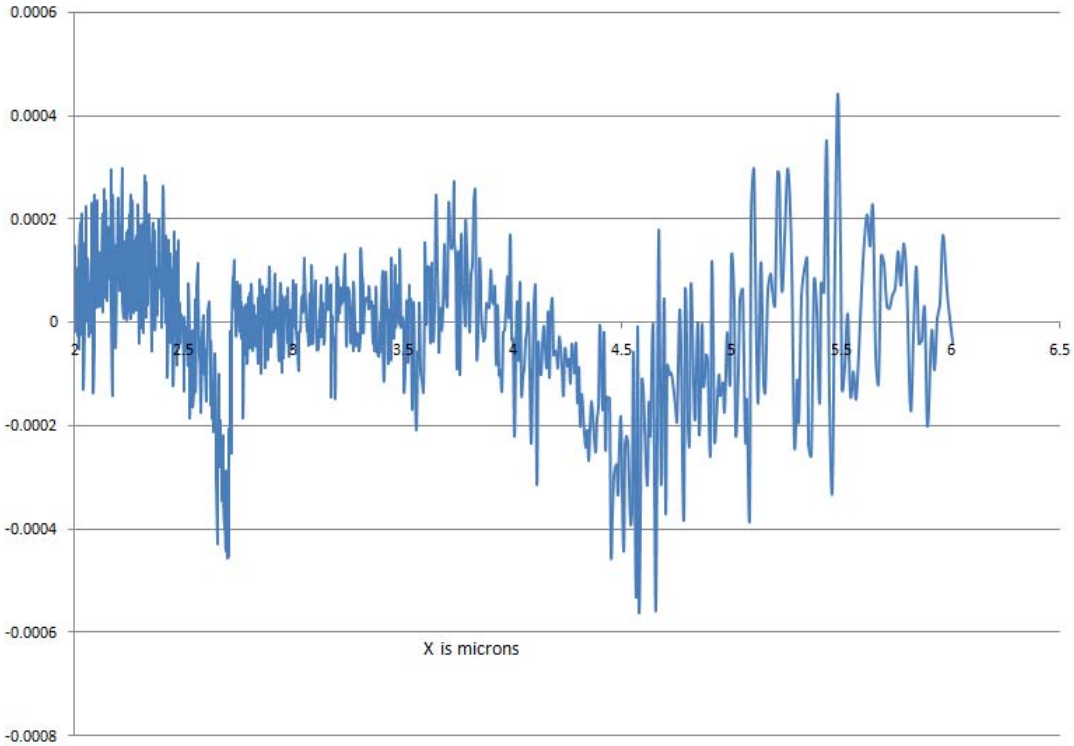

Fig: Estimation of 2-6 μm mid-infrared while spraying MIRGA atomizer

Supplementary text

T2: Detailed TEM interpretation

Bright-field images

Control sample:

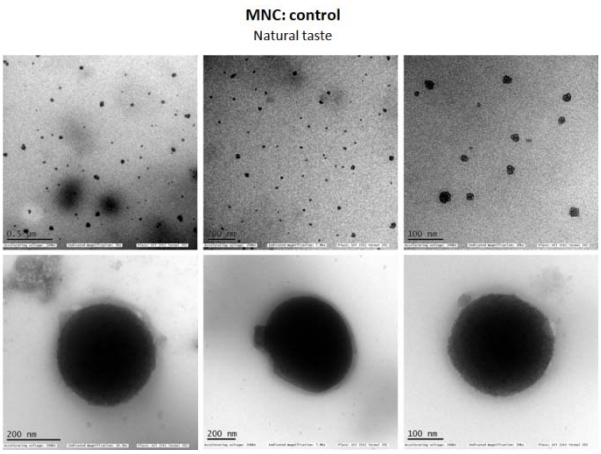

Top row images: nanoparticles. Bottom row images: submicron particles.

The control sample is mainly composed of particles, either in the nanometer (images in top row) and in the submicrometer (images in bottom row) ranges. Both particle types appear not clustered, each other or to other components, and show mainly semi-spherical shape. Size ranges are 10 – 30 nm for nanoparticles, and 300 – 400 nm for larger particles. Besides the size, main difference between the two types concerns the uniformity of distribution of the particle mass within particle body. In the nanoparticles the mass appear unevenly distributed, as it is mostly visible in top right image. Viceversa, larger particles show homogeneous mass distribution, as clearly documented by bottom row images. Dark appearance of particles has to be related to mass contrast, since the control sample has amorphous structure.

4 sprayed sample:

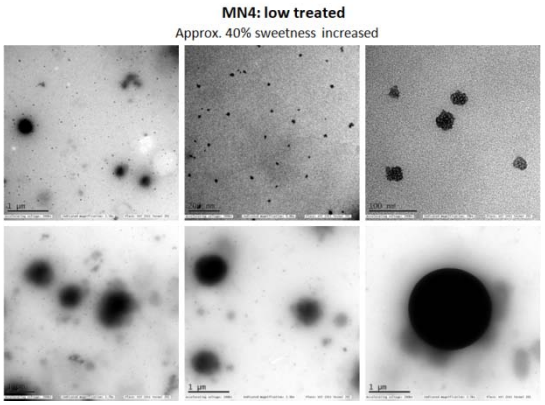

Top row images: nanoparticles. Bottom row images: particles in the submicrometer (left, central) and above-micrometer (right) ranges.

In the 4 sprayed sample the overall morphology of the control sample is preserved, indicating that the 4 sprayings does not affect heavily the sample matrix. It is mainly composed of particles, either in the nanometer (images in top row) and in the submicrometer (images in bottom row) ranges. Similarly to control, both particle types appear not clustered to other components, and show mainly semi-spherical shape. Size ranges are 10 – 30 nm for nanoparticles, and 100 – 400 nm for larger ones. An example of the combined presence of the two size ranges is given in top left image, where both nanoparticles and submicrometer particles are visible. However, differently from the control, larger particles are also observed, like the one in bottom right image, ranging 1 – 2 μm. Similarly to control, main difference between nanoparticles and larger particles concerns the distribution of mass within particle body. In the nanoparticles the mass appear unevenly distributed, as it is clearly visible in top right image. Viceversa, larger particles show homogeneous mass distribution, as clearly documented by bottom row images. Dark appearance of particles has to be related to mass contrast, since the 4 sprayed sample has amorphous structure.

10 sprayed sample:

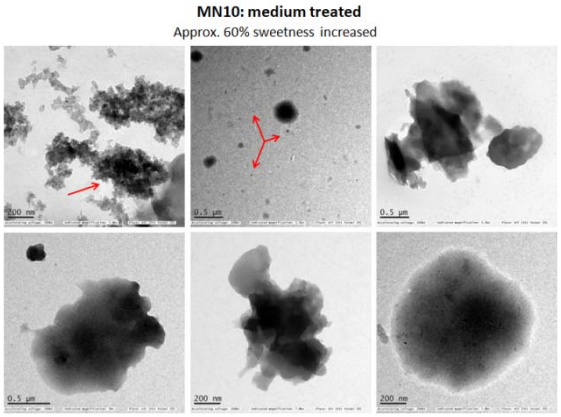

Top row images: clusters of nanoparticles (left), Bottom row images: particles in the submicrometer range (central), cluster of mass aggregates (right).

Semi-spherical nanoparticles similar to those observed in the control and 4 sprayed samples are anyway also visible in the 10 sprayed sample, like those indicated by arrows in the top central image. Amorphous-like aggregates of material range 0.5 – 2 μm size; they are observed either in clusters (top right image), or individually (bottom images). The inhomogeneous distribution of dark areas observed on these aggregates suggests an uneven distribution of mass within the aggregate body. Indeed, since also the 10 sprayed sample has non crystalline structure, dark areas have to be related to mass contrast effects.

14 sprayed sample:

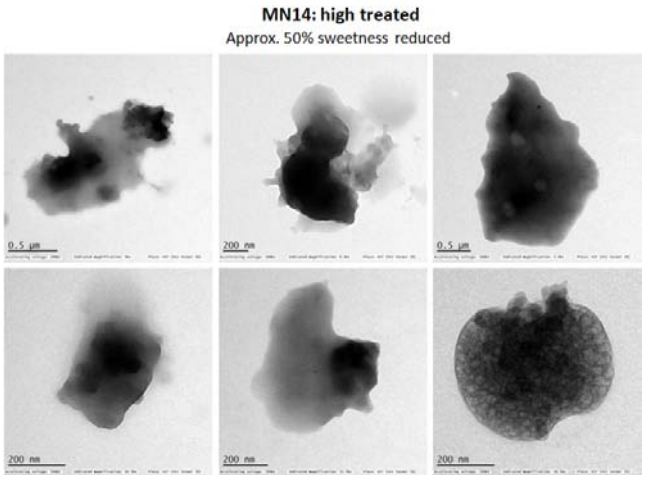

Top and bottom row images: different mass aggregates observed in this sample.

Differently from previously discussed samples, in the 14 sprayed sample the matrix structure and morphology of control is not preserved, indicating that also the 14 sprayings affects significantly the sample matrix itself. Neither nanoparticles, nor larger semi-spherical particles, are generally visible from available images, while mass aggregates are widely documented, suggesting that this type of materials are far more abundant than in previously discussed samples, with the partial exception of the medium treated one. Mass aggregates show similar size range than those of 10 sprayed sample. Similarly to the latter, also, a clearly inhomogeneous distribution of dark areas is observed on these aggregates, that suggests an uneven distribution of mass within the aggregate body. Indeed, since also the 14 sprayed sample has non crystalline structure, dark areas have to be related to mass contrast effects. Finally, a sponge-like mass distribution is observed in bottom right image that is not visible in previous samples.

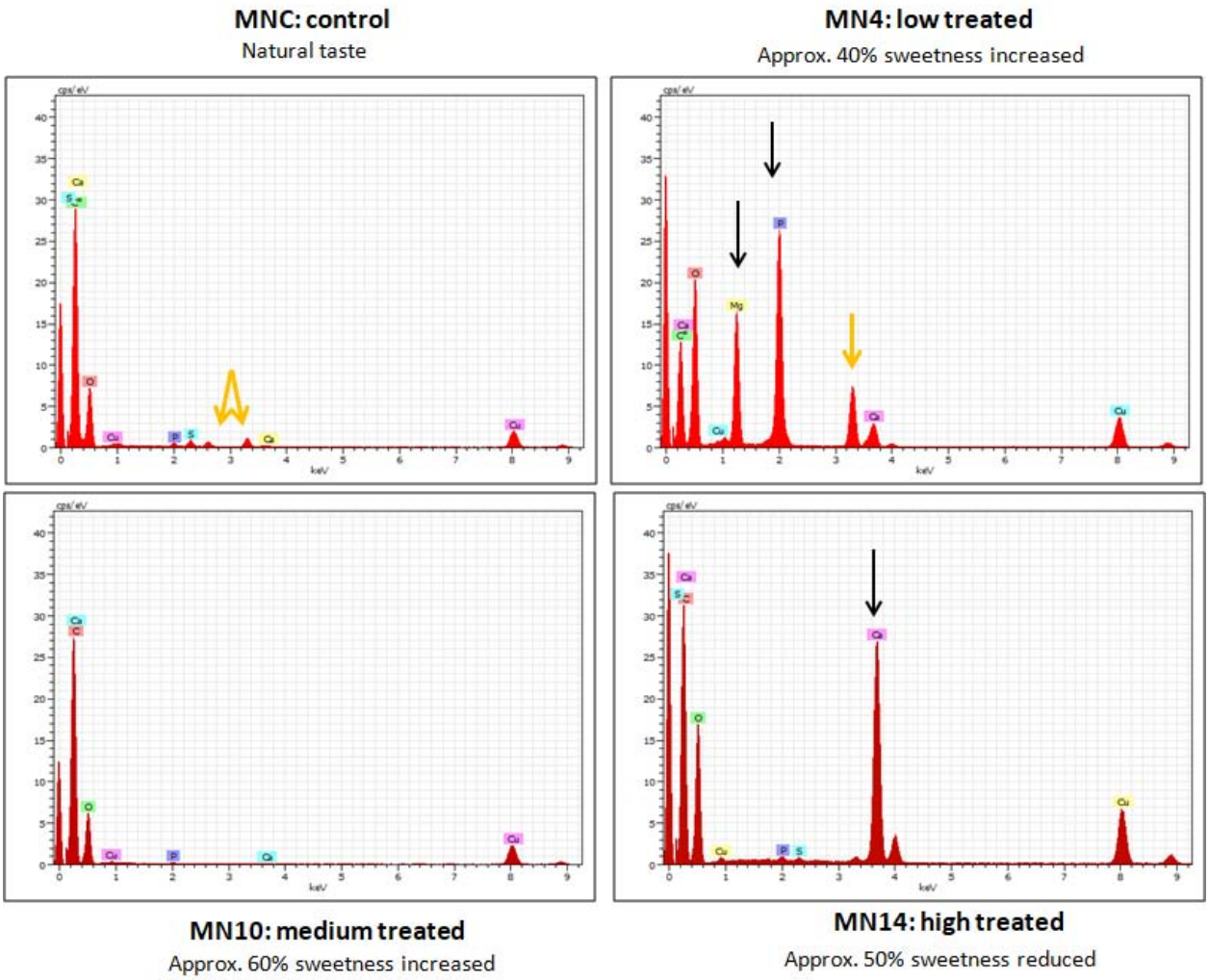

MNC: control
Natural taste

Spectrum: Spectrum 455-MNC

Element	Series	Net unn. C [wt.%]	norm. C [wt.%]	Atom. C [at.%]	Error (3 Sigma) [wt.%]
Oxygen	K-series	30331	3.59	3.59	2.78	0.40
Carbon	K-series	113161	93.88	93.88	96.64	8.57
Phosphorus	K-series	2205	0.15	0.15	0.06	0.09
Sulfur	K-series	4244	0.28	0.28	0.11	0.10
Copper	K-series	19011	2.01	2.01	0.39	0.26
Calcium	K-series	1195	0.08	0.08	0.03	0.09
Total:			100.00	100.00	100.00	

MN4: low treated
Approx. 40% sweetness increased

Spectrum: Spectrum 456-MN4

Element	Series	Net unn. C [wt.%]	norm. C [wt.%]	Atom. C [at.%]	Error (3 Sigma) [wt.%]
Oxygen	K-series	36194	14.37	14.37	13.77	1.39
Carbon	K-series	20457	56.87	56.87	72.60	5.33
Phosphorus	K-series	62247	14.35	14.35	7.10	1.38
Copper	K-series	14703	5.21	5.21	1.26	0.56
Calcium	K-series	8926	2.12	2.12	0.81	0.28
Magnesium	K-series	32221	7.08	7.08	4.46	0.72
Total:			100.00	100.00	100.00	

Spectrum: Spectrum 457-MN10

Element	Series	Net unn. C [wt.%]	norm. C [wt.%]	Atom. C [at.%]	Error (3 Sigma) [wt.%]
Carbon	K-series	125442	94.23	94.23	97.01	8.59
Oxygen	K-series	29842	3.20	3.20	2.47	0.37
Phosphorus	K-series	851	0.05	0.05	0.02	0.08
Calcium	K-series	539	0.03	0.03	0.01	0.08
Copper	K-series	25958	2.48	2.48	0.48	0.30
Total:			100.00	100.00	100.00	

MN10: medium treated
Approx. 60% sweetness increased

Spectrum: Spectrum 458-MN14

Element	Series	Net unn. C [wt.%]	norm. C [wt.%]	Atom. C [at.%]	Error (3 Sigma) [wt.%]
Carbon	K-series	48868	77.83	77.83	89.62	7.16
Oxygen	K-series	28455	6.47	6.47	5.59	0.67
Phosphorus	K-series	845	0.11	0.11	0.05	0.09
Sulfur	K-series	564	0.07	0.07	0.03	0.09
Calcium	K-series	76680	10.45	10.45	3.61	1.02
Copper	K-series	24936	5.06	5.06	1.10	0.54
Total:			100.00	100.00	100.00	

MN14: high treated
Approx. 50% sweetness reduced

To summarize, with respect to the control sample, 4 spraying affected the sample with minor changes of morphology and matrix structure. Conversely, both 10 and 14 sprayings affected significantly the sample morphology and matrix structure, with differences mainly in the type of particles observed: semi-spherical individual nanoparticles and submicrometer particles are observed as main

components of the control and 4 sprayed samples, while ellipsoidal nanoparticles grouped in large clusters and above-micrometer mass aggregates are observed in the 10 and 14 sprayed samples.

Supplementary text

T3: Detailed 1H-NMR interpretation

Control

δ 0.50-2.70). This is due to Aliphatic group.
δ 1.068-1.103.This is due to-β hydroxybutyrate GROUP.
δ 2.508 This is due to DMSO-d6.
δ 3.372.This is due to H2O peak.
δ 2.70-3.90.This is due to sugar ring and residual water proton.
δ 3.90-6.00This is due to sugar ring –OH and –NH protons.
δ 5.12-5.96.This is due to CARBOHYDRAT anomeric proton.

4 sprayed

δ 0.50-2.70). This is due to Aliphatic group.
δ 1.068-1.103.This is due to-β hydroxybutyrate GROUP.(Intensity is very less in comparision to control)
δ 2.508 This is due to DMSO-d6.
δ 3.372.This is due to H2O peak.
δ 2.70-3.90.This is due to sugar ring and residual water proton.
δ 3.90-6.00This is due to sugar ring –OH and –NH protons.(This is absent in this sample)
δ 5.12-5.96.This is due to CARBOHYDRAT anomeric proton.(This peak is absent)

10 sprayed

δ 0.50-2.70). This is due to Aliphatic group.
δ 1.068-1.103.This is due to-β hydroxybutyrate GROUP.
δ 2.508 This is due to DMSO-d6.
δ 3.372.This is due to H2O peak.
δ 2.70-3.90.This is due to sugar ring and residual water proton.
δ 3.90-6.00This is due to sugar ring –OH and –NH protons.
δ 5.12-5.96.This is due to CARBOHYDRAT anomeric proton.

14 sprayed

δ 0.50-2.70). This is due to Aliphatic group.
δ 1.068-1.103.This is due to-β hydroxybutyrate GROUP.
δ 2.508 This is due to DMSO-d6.
δ 3.372.This is due to H2O peak.
δ 2.70-3.90.This is due to sugar ring and residual water proton.
δ 3.90-6.00This is due to sugar ring –OH and –NH protons.
δ 5.12-5.96.This is due to CARBOHYDRAT anomeric proton.

Supplementary text

T4: Detailed discussion

1. *Detailed discussion [1]*

1.1. Invention background

The four observable states of matter (solid, liquid, gas, and plasma) are composed of intermolecular and intramolecular bonds. The inherent characteristics of neutrons, protons and electrons are unique, however, differences in their numbers are what constitute different atoms, and how these atoms bind together develops into different molecules with unique characteristics. In the electromagnetic wave (EMW) spectrum, the mid-IR region is vital and interesting for many applications since this region coincides with the internal vibration of most molecules [2]. Almost all thermal radiation on the surface of the Earth lies in the mid-IR region, indeed, 66% of the Sun's energy we receive is infrared [3] and is absorbed and radiated by all particles on the Earth. At the molecular level, the interaction of mid-IR wavelength energy elicits rotational and vibrational modes (from about 4500–500 cm^{-1}, roughly 2.2 to 20 microns) through a change in the dipole movement, leading to chemical bond alterations [4].

During our research we have observed: *(A)* In all objects, even though atoms always remain as atoms, their chemical bond parameters are continuously prone to alteration by cosmic and physical energies (e.g.: EMW, heat, pressure, and humidity) causing the bonds to compress/stretch/bend [5-8], break [9,10], or new bonds to be formed [11]. These alterations ultimately lead to changes in the physicochemical characteristics of the objects. *(B)* The dynamic, constant, and mutual influences of EMW among the Earth and the celestial and living bodies are continuously causing alterations in the inherent physiochemical characters of earthly objects, for instance, enhancement due to an optimum

dose of energy or decrease/destruction due to a high dose of energy (detailed below). Thus, based on these concepts, MIRGA was developed to alter the bond parameters, thereby potentiating the natural characteristics of products.

1.2. *MIRGA definition*

We define MIRGA as *'a harmless, economical atomizer containing an imbalanced ratio of ions suspended in water, which influence the natural potency of target substances by generating mid-IR while spraying'*.

1.3. *Technique of mid-IR generation from MIRGA*

We designed MIRGA as to accommodate an imbalanced ratio of ions suspended in water in their fundamental state, which can move as free particles. The solution exhibits very little detectable background frequency, below even that of cosmic events. By comparison humans emit more radioactivity (around 10 microns) [12,13]. We designed MIRGA to generate energy based on various processes such as: (A) spraying leads to ionization (electrons getting separated from atoms) and many pathways for electron re-absorption; due to these two oscillatory processes, energy is generated; (B) while spraying, a water-based ionic solution gets excited/charged, which in turn leads to oscillation among the imbalanced ions [14] in their excited state, resulting in the emission of photons [15,16]; (C) although a low electromagnetic field exists between the charged particles of the MIRGA's ionic solution, during spraying the induced oscillation between these charged particles produces energy [17-21]; and (D) in the natural rainfall process, more energy is required to break the water bonds for creating smaller water droplets [22]. Therefore, these droplets should have more stored energy, which then travels down at velocity from a specific distance, thus gaining kinetic energy. When the rain hits the Earth's surface, it forms a very thin film of mid-IR (nearly 6 micron), hence there is a net heat gain [22,23]. We simulated this rainfall's energy-gaining process in MIRGA(i.e., when imbalanced ions in liquid media are atomized, the ejected smaller droplets should have higher internal energy as well as acquired kinetic energy, and the energy emitted by breaking the surface tension). From trial and error, we calibrated the ejection pressure to obtain a desired fine mist, and minimized the evaporation rate by altering the pH and density of the solution. Moreover, the accelerated ions in the sprayed ionic clouds collide among themselves and generate energy [24], thus, we incorporated these phenomena in our atomizer and designed it in such a way as to emit energy in the 2–6 μm mid-IR depending on the given plunger pressure.

Yousif et al. [25] described this process as a photo dissociation of molecules caused by the absorption of photons from sunlight, including those of infrared radiation, visible light, and ultraviolet light, leading to changes in the molecular structure.

1.4. *Safety of MIRGA-sprayed products*

In our nearly two-decades of research, we have observed that MIRGA-induced bond-altered target substances do not show any adverse reaction upon consumption/use. In nature, *(A)* Stereochemical configuration has great influence on taste [26] (e.g., varieties of mango, grapes, rice, etc.), *(B)* Cooking and digestive enzymes break chemical bonds, thereby softening foods. This indicates that alterations in chemical bonds occur naturally and do not represent a risk to human health. As an example, boiledrice, puffed rice, flat rice, and rice flour have a unique aroma, taste, texture, and shelf-life but conserving the same molecular formula ($C_6H_{10}O_5$). *(C)* In the food industry, sensory attributes and shelf-life are enhanced by altering the food's chemical bonds using various irradiation processes like radappertization, radicidation, and radurization [27]. *(D)* Uponheating, water changes from ice to liquid to steam, which are manifestations of changes in the hydrogen bonds [28] but the chemical composition (H_2O) remains the same [29].

1.5. *MIRGA's primeval and future scope*

The water-based MIRGA could be the first novel potentiating technology. This type of atomizer technology also seems to be present with the extra-terrestrials for their therapeutic use during visitations [30].

In various products, we have achieved a range from 30% to 173% potentiation. Even the smaller improvement resulted in 30% monetary and resource savings as well as health benefits. However, there is a knowledge gap between potentiation from 30% to at least 100% for all products, which can be filled-up by refining MIRGA's ionic solution, concentration, atomizer pressure, and other parameters and even formulating a better solution.

Various mid-IR emitters are now available (e.g., silicon photonic devices [31], cascade lasers quantum and interband [32], non-cascade-based lasers, chalcogenide fiber-based photonic devices [33], and suspended-core tellurium-based chalcogenide fiber photonic devices [34]). These emitters are not as cost-effective as MIRGA and are useful only in astronomy, military, medicine, industry, and research applications. These emitters are too complex for domestic application by the average user.

Because of MIRGA's wide range of applications, we believe that this technique will resonate in many scientific fields including biophotonics, therapeutics, health, ecology, and others. We are currently conducting research on MIRGA and its applications, namely MIRGA salt, MIRGA vapor and MIRGA plasma.

References Références Referencias

1. Umakanthan, Mathi M, 2022. Decaffeination and improvement of taste, flavor and health safety of coffee and tea using mid-infrared wavelength rays. Heliyon, e11338, Vol 8(11). doi: 10.1016/j.heliyon.2022.e11338
2. CORDIS, European commission. New advances in mid-infrared laser technology, Compact, high-energy, and wavelength-diverse coherent mid-infrared source. Available at: https://cordis.europa.eu/project/rcn/99977/brief/en (last accessed on 27.01.2019)
3. A. Salam, A. Ammar, A.H. Asaad, L. Yi-Chen, C. Francesco, 2019. Molecules A Comprehensive Review on Infrared Heating Applications in Food Processing. Molecules. 24, 2-21. doi: 10.3390/molecules24224125.
4. J. E. Girard, Principles of Environmental Chemistry, third ed., Jones & Bartlett Learning, USA, 2014, pp. 99.
5. James E. Girard, 2014. Principles of Environmental Chemistry, 3rd edition, Jones & Bartlett Learning, USA, p99
6. Avelion Alvarez and Miguel Prieto, 2012. Fourier Transform Infrared spectroscopy in Food Microbiology, Springer Science & Business Media, p3.
7. Brian C. Smith. Infrared Spectral Interpretation: A Systematic Approach, CRC Press, LLC, 7, (1999)
8. Dwivedi Ravi Shankar, 2017. Remote Sensing of Soils. Germany: Springer-Verlag GmbH, p268
9. Jag Mohan. Organic Spectroscopy: Principles and Applications, 2nd edition, Alpha science international Ltd., Harrow, UK, 19, (2004). Available at: https://books.google.co.in/books?id=fA08Uy5DR0QC&printsec=frontcover&dq=Jag+Mohan.+Organic+Spectroscopy:+Principles+and+Applications&hl=en&sa=X&ved=0ahUKEwjHpcHUi9fgAhXXFIgKHXvRCpIQ6AEIKjAA#v=onepage&q=Jag%20Mohan.%20Organic%20Spectroscopy%3A%20Principles%20and%20Applications&f=false
10. Carolyn McMakin, 2011. Frequency specific Microcurrent in pain management E-book, Elsevier, China, p 30.
11. David Moss, 2011. Biomedical Applications of Synchrotron Infrared Microspectroscopy: A Practical Approach, Royal Society of Chemistry, UK, p 58.
12. Peter H. Raven, Linda R. Berg, David M. Hassenzahl, 2012. Environment, John Wiley & Sons, Inc., USA, p45. Available at: https://books.google.co.in/books?id=QVpO2R51JBIC&pg=RA1-PA45&dq=electromagnetic+waves+make+form+new+bonds&hl=en&sa=X&ved=0ahUKEwiTnO2amMbjAhUJ3o8KHSfkAJEQ6AEIMjAB#v=onepage&q=electromagnetic%20waves%20make%20form%20new%20bonds&f=false
13. Frances Ashcroft, 2000. Life at the Extremes: The Science of Survival, University of California Press, California, p122
14. Robert H. Sanders, 2014. Revealing the Heart of the Galaxy, Cambridge University Press, USA, p70
15. Frank Verheest. Waves in Dusty Space Plasmas, Kluwer Academic Publishers, Netherlands, 89, (2000)
16. Sun Keping, Gefei Yu. Recent developments in Applied Electrostatics (ICAES2004): Proceedings of the Fifth International Conference on Applied Electrostatics, Elsevier Ltd., UK, p87.
17. Pierre L. Fauchais, Joachim V.R. Heberlein, Maher I. Boulos. Thermal Spray Fundamentals From Powder to Part. Springer Science & Business Media, New York, 84 (2014)
18. Manfred Wendish, Jean-Louis Brenguier. Airborne Measurements for environmental Research: Methods and Instruments, Wiley-VCH. Available at: https://books.google.co.uk/books?id=tHdwhn-c5mgC&pg=PT419&dq=A+regularly+oscillating+charge+produces+a+harmonic+electromagnetic+waves+Manfred&hl=en&sa=X&ved=0ahUKEwjBqdv75tvgAhWpSxUIHbQ_D0gQ6AEIKjAA#v=onepage&q=A%20regularly%20oscillating%20charge%20produces%20a%20harmonic%20electromagnetic%20waves%20Manfred&f=false (last accessed on 27.02.2019)
19. Kongbam Chandramani Singh, 2009. Basic Physics, PHL Learning Private Limited, New Delhi, p413
20. Mathura Prasad. Soul, God and Buddha in Language of Science, Notion Press, Chennai(2017)
21. Stephen Pople, 1999. Complete Physics, Oxford University Press, Oxford, p166
22. Roger Barry, Richard Chorley, 1998. Atmosphere, Weather and Climate, 7th edition, Routledge, London, p51
23. Eniday: https://www.eniday.com/en/sparks_en/harnessing-the-energy-of-rain/ (last accessed on 06.02.2019)
24. Krishnakumar, T (2019). Application of Microwave Heating In Food Industry. 10.13140/RG.2.2.27035.72488.
25. Yousif, E., & Haddad, R. (2013). Photodegradation and photostabilization of polymers, especially polystyrene: review. SpringerPlus, 2, 398. https://doi.org/10.1186/2193-1801-2-398
26. Kenneth L., Williamson, Katherine M. Masters, 2011. Macroscale and Microscale Organic Experiments, 6th edition, Brooks/ Cole C engage learning, CA, p720
27. Sivasankar B. Food Processing and preservation, PHI Learning Private Limited, Delhi, 246, (2014)
28. Trevor Day, 1999. Ecosystems: Oceans. Routledge Taylor & Francis Group, London and New York, p44

29. Kenneth W. Raymond, 2010. General Organic and Biological Chemistry, 3rd edition, John Wiley & Sons, Inc., USA, p176
30. Blue planet project: Alien Technical research–25, Westchester Camp, Office of the Central Research #3. CODE: ARAMISIII–ADR3-24SM, p80-81
31. CMOS Emerging Technologies. CMOSET 2012: Abstracts, p49. Available at: https://books.google.co.in/books?id=3XVYC-yBgksC&pg=PA49&dq=mid+infra#v=onepage&q&f=false
32. Jung, D., Bank, S., Lee, M. L., & Wasserman, D. (2017). Next-generation mid-infrared sources. Journal of Optics, 19(12), 123001. doi: 10.1088/2040-8986/aa939b.
33. Sincore, A. & Cook, Justin & Tan, Felix & El Halawany, Ahmed & Riggins, A. & McDaniel, S. & Cook, G. & Martyshkin, Dmitry & Fedorov, V.V. & Mirov, Sergey & Shah, L. & Abouraddy, A. & Richardson, M. & Schepler, Kenneth. (2018). High power single-mode delivery of mid-infrared sources through chalcogenide fiber. Optics Express, 26(6), 7313. doi:10.1364/oe.26.007313.
34. Wu, Bo & Zhao, Zheming & Wang, Xunsi & Tian, Youmei & Mi, Nan & Chen, Peng & Xue, Zugang & Liu, Zijun & Zhang, Peiqing & Shen, Xiang &Nie, Qiuhua & Dai, Shaocong & Wang, R.P. (2018). Mid-infrared supercontinuum generation in a suspended-core tellurium-based chalcogenide fiber. Optical Materials Express, 8(5), 1341. doi: 10.1364/ome.8.001341.